J Mol Model (2009) 15:515–523
DOI 10.1007/s00894-008-0415-8

ORIGINAL PAPER

A theoretical study on unusual intermolecular T-shaped X–H...π interactions between the singlet state HB=BH and HF, HCl, HCN or H_2C_2

Fu-de Ren · Duan-lin Cao · Wen-liang Wang · Jun Ren · Su-qing Hou · Shu-sen Chen

Received: 7 July 2008 / Accepted: 27 July 2008 / Published online: 17 December 2008

Abstract The unusual T-shaped X–H...π hydrogen bonds are found between the B=B double bond of the singlet state HB=BH and the acid hydrogen of HF, HCl, HCN and H_2C_2 using MP2 and B3LYP methods at 6-311++G(2df,2p) and aug-cc-pVTZ levels. The binding energies follow the order of HB=BH...HF>HB=BH...HCl>HB=BH...HCN>HB=BH...H_2C_2. The hydrogen-bonded interactions in HB=BH...HX are found to be stronger than those in H_2C=CH_2...HX and OCB≡BCO...HX. The analyses of natural bond orbital (NBO) and the electron density shifts reveal that the nature of the T-shaped X–H...π hydrogen-bonded interaction is that much of the lost density from the π-orbital of B=B bond is shifted toward the hydrogen atom of the proton donor, leading to the electron density accumulation and the formation of the hydrogen bond. The atoms in molecules (AIM) theory have also been applied to characterize bond critical points and confirm that the B=B double bond can be a potential proton acceptor.

F.-d. Ren (✉) · D.-l. Cao · J. Ren · S.-q. Hou
College of Chemical Engineering and environment,
North University of China,
Taiyuan 030051, China
e-mail: fdren888@126.com

F.-d. Ren
Library of North University of China,
Taiyuan 030051, China

W.-l. Wang
School of Science, Beijing Institute of Technology,
Beijing 100081, China

S.-s. Chen
School of Chemistry and Materials Science,
Shaanxi Normal University,
Xi'an 710062, China

Keywords B=B double bond · Electron density shifts · T-shaped X–H...π hydrogen bond

Introduction

Recently T-shaped X–H...π hydrogen bonds have received much attention in experimental studies and theoretical calculations as a result of their extremely important role in determining the structures and activities of organic, organometallic and biological molecules as well as the reaction mechanism of the electrophilic addition to the triple or double bonds [1–17]. It has been extensively shown from many experimental and theoretical results that the T-shaped X–H...π hydrogen bonds can be established between triple and double bonds, aromatic and cyclopropane rings as proton acceptors, and X–H compounds (hydrogen halides, O–H, N–H, C–H derivatives, etc.) [3–17]. In particular, very recently this kind of T-shaped X–H...π hydrogen bonds have also been found between the B≡B triple bond composed of the electron-deficient atoms and the acid hydrogen of HF, HCl, HCN and H_2C_2 [18]. This theoretical result has revealed that the B≡B triple-bond undergoes unusual contraction upon the T-shaped X–H...π hydrogen-bond formation. Furthermore, the analyses of the charge density and electron density shifts have explained the origin of the B≡B bond contraction and confirmed that the B≡B triple-bond can be as potential proton acceptor [18]. However, for the novel B=B double bond as the proton acceptor, to our knowledge, no investigation on the T-shaped X–H...π hydrogen bond has been presented.

For a long time, the B_2H_2 molecule has been of great chemical interest because of the nature of the B–B bond that the electron-deficient nature of boron hinders the formation of the double-bond [19–27]. Knight et al. [19]

reported the first definitive experimental characterization of this species by electron spin resonance in neon and argon matrices at 4 K and carried out the CI calculations of the hyperfine constants for the singlet state $^1\Delta_g$ of the $D_{\infty h}$ point group, and Jouany et al. [22] investigated the low-lying states $^1\Delta_g$ by means of CI calculations using a double-zeta basis set. They found the valence molecular orbitals of B_2H_2 were $(2\sigma_g)^2(2\sigma_u)^2(3\sigma_g)^2(1\pi_u)^2$ where the first two σ type orbitals involved bonding and antibonding boron 2s electrons and the two paired electrons occupied degenerate boron p bonding orbitals, indicating that it contained one B–B π bonding orbital [19]. Furthermore, Jouany et al. [22] found an equilibrium B–B bond length of 1.498 Å, suggesting that the shortening of the B–B bond length (0.186 Å) with respect to the corresponding value in B_2H_4 was attributed to the double-bond character of the B–B bond in B_2H_2. Thus, the B=B double-bond character in the singlet state B_2H_2 was confirmed. It is generally known that, due to the relative stronger fluidity of the π-electrons, the π orbital might cause the H-bond acceptor behavior to form the T-shaped X–H...π hydrogen bond. Then for the unusual electron deficient B=B double-bond, can it provide π-electrons and be as the potential proton acceptor to form the T-shaped X–H...π hydrogen bond?

In this paper, our goal is to study the unusual T-shaped X–H...π (X=F, Cl, CN, CCH) hydrogen-bonded interaction between the B=B double bond and the acid hydrogen. For this kind of novel T-shaped X–H...π hydrogen bond, theoretic investigation will reveal the nature of the interaction to further study on structures and activities for organic, organometallic and biological molecules involving the B=B double bonds, as well as the reaction mechanism of the electrophilic addition to the B=B double bond. These must be very useful for proposing the complexes of the B=B double bond as the proton acceptor in theory and experiment, akin to the C=C double-bond complexes.

Computational methods

It is well established that high-level quantum chemical calculations with electron correlation and large basis set including both diffuse and polarization functions are crucial to adequately describe molecular properties of weakly bound hydrogen-bonded complexes [28–29]. Firstly, it is necessary to reproduce various electric properties of the monomers as accurately as possible. This will ensure a correct description of the long-range interactions in the complex. Secondly, the sensitivity of these electric properties to the approach of the partner's orbitals should be minimized in order to diminish the basis set extension effects. Furthermore, the augmented correlation-consistent polarized valence-triple-ζ (aug-cc-pVTZ) basis set has been successfully applied in order to understand the nature of the T-shaped X–H...π hydrogen bonding as well as changes in the structural, electronic and vibrational properties after molecular complexation [12, 30–31]. So we decided to use the MP2 and B3LYP methods with 6-311++G(2df,2p) and aug-cc-pVTZ atomic basis sets in this investigation.

All the calculations have been performed using Gaussian 03 programs in Shaanxi Normal University [32]. All the possible T-shaped X–H...π hydrogen-bonded complexes have been fully optimized using MP2 and B3LYP methods with the 6-311++G(2df,2p) and aug-cc-pVTZ basis sets and the four complexes corresponding to the minimum energy points, at which the harmonic frequency analyses have been carried out and the complexes have no imaginary frequency, at the molecular energy hypersurface have been obtained. The natural bonding analysis [33] has also been carried out at B3LYP/aug-cc-pVTZ. The shifts of the electron densities [34] that accompany formation of the T-shaped X–H...π H-bonds have been displayed at MP2/aug-cc-pVTZ level using GaussView program and the topological electron charge density has been analyzed by the atoms in molecules (AIM) method [35] using AIMPAC program [36] at the same level. The frequency shifts ($\Delta\nu$), defined as the difference between the frequency of the certain vibrational mode in the complex and it in isolated molecule, can be expressed as follows:

$$\Delta\nu = \nu_{complex} - \nu_{monomer}$$

Binding energy (D_e) is defined as:

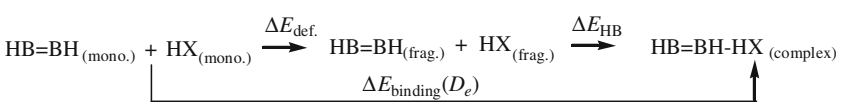

Because the deformation energy ($\Delta E_{def.}$), defined as the energy difference between the isolated molecule and the molecular framework at the geometry of the complex, is negligible for T-shaped hydrogen-bonded structure [9–13,

17–18], the value of H-bond energy (ΔE_{HB}) is almost equal to that of the binding energy (D_e). So for these systems it can be expressed as follows:

$$D_e = E_{(HB=BH-HX)complex} - E_{(HB=BH)mono.} - E_{(HX)mono.},$$

The D_e corrected for the basis set superposition error (BSSE) [37, 38] and zero-point energy correction (ZPEC) was evaluated.

Results and discussion

Four complexes are obtained and their fully optimized geometries, the bond critical points (BCPs), and atomic labels are shown in Fig. 1. The geometries parameters and the electron densities at the BCPs are listed in Table 1. The binding energies are presented in Table 2. Frequency shifts of the monomers in complexes and the results of the natural bond orbital (NBO) analysis are in Tables 3 and 4, respectively, and the shifts of electron densities are illustrated in Fig. 3. The unusual T-shaped X–H...π hydrogen bonds are found between the B=B double bond of the singlet state HB=BH and the acid hydrogen of HF, HCl, HCN or H_2C_2. The binding energies follow the order of HB=BH...HF>HB=BH... HCl>HB=BH…HCN>HB=BH…H_2C_2. The analyses of the charge density and electron density shifts confirm that the B=B double bond can be a potential proton acceptor.

Geometry of the complex

As can be seen from Fig. 1, the X–H...π hydrogen bond is found, and each forms a C_{2V} T-shape with the X–H lying perpendicular to the B=B double bond and pointing toward to its midpoint. To improve the reliability of the results on this kind of novel T-shaped hydrogen bond, the comparisons of the structures with the analogous H_2C=CH_2...HX complexes containing double bond are carried out at MP2/aug-cc-PVTZ level.

Form Table 1, for HB=BH...HF, the increment of the F6–H5 bond length is increased by 0.019 Å, whereas the corresponding value in H_2C=CH_2...HF is only increased by 0.010 Å, showing that the increment of the F6–H5 bond distance in HB=BH...HF is larger than that in H_2C=CH_2... HF by 0.009 Å at MP2/aug-cc-PVTZ level. Furthermore, the distance of H5...π hydrogen bond is 2.183 Å whereas the corresponding value in H_2C=CH_2...HF is 2.129Å, only greater than that in H_2C=CH_2...HF by 0.054 Å at MP2/aug-cc-PVTZ level. These results indicate the complex might acquire a T-shaped F–H...π hydrogen-bonded geometry.

Akin to the HB=BH...HF complex, the T-shaped Cl–H...π hydrogen bond in HB=BH...HCl is also found according to the increment of the Cl6–H5 bond length in HB=BH...HCl lower than that in H_2C=CH_2...HCl at MP2/aug-cc-PVTZ level. The increment of the Cl6–H5 bond length is increased by 0.023 Å in HB=BH...HCl whereas the corresponding value in H_2C=CH_2...HCl is only elongated by 0.011 Å, indicating that it is two times larger in HB=BH...HCl than that in H_2C=CH_2...HCl. The distance of H5...π hydrogen bond, up to 2.343 Å, is just greater than that in H_2C=CH_2...HCl (2.297 Å) by 0.046, suggesting the possible Cl–H...π hydrogen bond in the HB=BH...HCl complex.

For the typical proton donors HCN and H_2C_2, the T-shaped X–H...π hydrogen bond can also not be neglected. Indeed, it is also observed in both HB=BH...HCN and HB=BH...H_2C_2 from Table 1 and Fig. 1. The distance of C6–H5 in proton donor is lengthened from 1.064 to 1.072 Å in HB=BH... HCN and from 1.062 to 1.066 Å in HB=BH...H_2C_2 at MP2/aug-cc-PVTZ level, respectively, analogously greatly to what is verified in H_2C=CH_2...HCN and H_2C=CH_2...H_2C_2 (from 1.064 to 1.070 Å and from 1.062 to 1.066 Å, respectively). Moreover, the distance of H5...π hydrogen bond in HB=BH...HCN or HB=BH...H_2C_2, up to 2.742 or 2.883 Å, is slightly greater than that in H_2C=CH_2...HCN (2.540 Å) or H_2C=CH_2...H_2C_2 (2.645 Å).

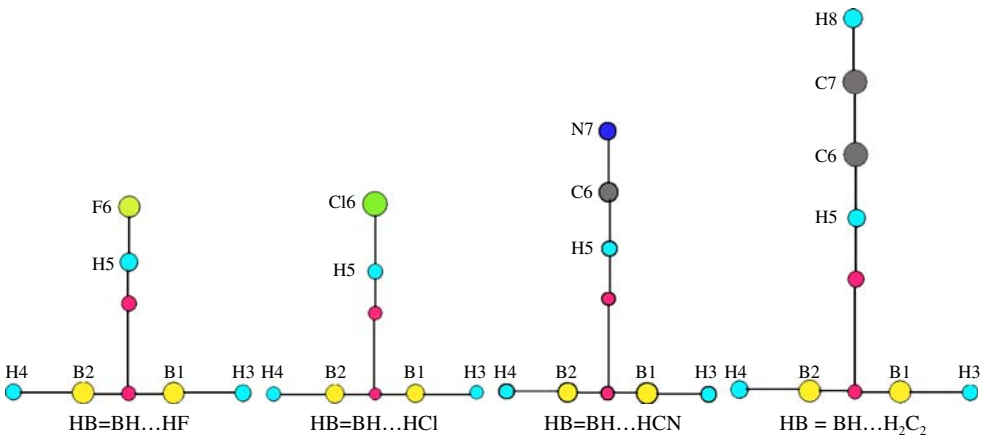

Fig. 1 Molecular structures for the four complexes. Small red spheres (unlabeled) represent bond critical points

Table 1 Principal geometry parameters (distances are in Å and angles are in degree) and selected bond critical point properties (in au) for HB=BH and complexes

parameters	HB = BH		HB = BH...HF		HB = BH...HCl		HB = BH...HCN		HB = BH...H_2C_2	
R(H5...π)			2.180[a]	2.181[b]	2.363[a]	2.371[b]	2.838[a]	2.838[b]	3.070[a]	3.062[b]
			2.209[c]	2.183[d]	2.365[c]	2.343[d]	2.775[c]	2.742[d]	2.946[c]	2.883[d]
R(B1=B2)	1.520[b]	1.530[d]	1.523[b]	1.532[d]	1.523[b]	1.532[d]	1.521[b]	1.531[d]	1.521[b]	1.530[d]
R(X6–H5)			0.946[b]	0.941[d]	1.313[b]	1.298[d]	1.073[b]	1.072[d]	1.066[b]	1.066[d]
R(X–H)[e]			0.924[b]	0.922[d]	1.284[b]	1.275[d]	1.066[b]	1.064[d]	1.062[b]	1.062[d]
ρ_{BCP}(H...π)[f]			0.0232		0.0203		0.0098		0.0075	
$\nabla^2\rho_{BCP}$(H...π)[f]			0.0329		0.0289		0.0209		0.0175	
ρ_{BCP}(B=B)[f]	0.1997		0.1982		0.1986		0.1991		0.1992	
$\nabla^2\rho_{BCP}$(B=B)[f]	-0.5863		-0.5568		-0.5783		-0.5821		-0.5823	

[a] Calculated values at B3LYP/6-311++G(2df,2p) level
[b] At B3LYP/aug-cc-PVTZ level
[c] At MP2/6-311++G(2df,2p) level
[d] At MP2/aug-cc-PVTZ level
[e] Calculated values of X–H bond for isolated HX
[f] At MP2/ aug-cc-PVTZ level

Interestingly, different from the complexes OCB≡BCO...HX, in which the B≡B triple bond undergoes contraction as a result of T-shaped X–H...π hydrogen-bonded interaction [18], the B=B double bond was slightly elongated from 1.520 to 1.523, 1.523, 1.521 and 1.521 Å for the four complexes at B3LYP/aug-cc-PVTZ level, respectively.

As can be seen from Table 1, the distance of H...π hydrogen bond is the same order of HB=BH...H_2C_2>HB=BH...HCN>HB=BH...HCl>HB=BH...HF at four levels, suggesting that the strength of T-shaped X–H...π hydrogen bond in HB=BH...HF is greatest while it is poorest in HB=BH...H_2C_2. On the other hand, the increment of the X6–H5 bond distance in HB=BH...HX is larger than the corresponding value in H_2C=CH_2...HX at MP2/aug-cc-PVTZ level, showing that the intermolecular T-shaped X–H...π hydrogen-bonded interactions in HB=BH...HX might be stronger than those in H_2C=CH_2...HX.

Binding energies and stabilities

Table 2 gives both uncorrected and corrected binding energies after correction of the ZPE and BSSE by means of the counterpoise method. For the complex HB=BH...HF, the interaction energy after correction of the BSSE amounts to 25.80 and 27.97 kJ/mol at MP2/6-311++G(2df,2p) and MP2/aug-cc-pVTZ levels, respectively, while for HB=BH...H_2C_2, the interaction energy is just equal to 7.02 and 7.73 kJ/mol after correction of the BSSE. There is no direct measure of the interaction energy for the system, but there is value reported in the literature of 3.36 kcal/mol (i.e., 14.05 kJ/mol) employing MP2/6-311++G** method after correction of the BSSE for the C_2H_4...HF complex [4]. Furthermore, in our previous investigations on T-shaped X–H...π hydrogen-bonded interactions between the B≡B triple bond and the acid hydrogen, the interaction energy after correction of the BSSE amounts to 13.76 and 12.21 kJ/mol with MP2/6-311++G(2d,p) and MP2/aug-cc-pVTZ methods, respectively, whereas for OCB≡BCO...H_2C_2, it is just 4.34 and 5.99 kJ/mol [18]. In particular, many investigations on T-shaped X–H...π hydrogen-bonded interactions have revealed that, in general, this kind of interaction energy is around 3.0 kcal/mol (i.e., 12.54 kJ/mol) [4]. Comparing the result mentioned above with the data listed in Table 3, it can be seen that the calculated results are reliable. Moreover, the interaction energy in the complex between the B=B double bond of the singlet state HB=BH and HX is much higher than that in the complex between the B≡B triple bond and HX.

Table 2 Binding energies of complexes ($-D_e$ (kJ/mol))

parameters	MP2/6-311++G(2df,2p)			MP2/aug-cc-pVTZ		B3LYP/6-311++G(2df,2p)			B3LYP/aug-cc-pVTZ		
HB=BH...HF	29.33	(25.80)[a]	16.67[b]	30.49	(27.97)[a]	30.05	(28.73)[a]	20.60[b]	29.10	(28.81)[a]	21.09[b]
HB=BH...HCl	21.20	(17.61)	10.41	22.00	(19.73)	18.32	(16.73)	9.80	17.16	(16.92)	11.08
HB=BH...HCN	14.00	(12.31)	6.01	14.88	(13.13)	10.95	(10.45)	4.65	10.79	(10.51)	5.04
HB=BH...H_2C_2	8.41	(7.02)	1.50	9.20	(7.73)	5.00	(4.57)	0.85	4.82	(4.61)	0.50

[a] The value in the parentheses is BSSE-corrected ($-D_{e(BSSE)}$)
[b] The binding energy is ΔE with BSSE and ZPE ($-D_{e(BSSE,\ ZPE)}$) correction

Table 3 Selected frequency shifts relative to the monomers for the complexes and IR intensities in the complexes at MP2/6-311++G (2df,2p) level[a]

	HB=BH		HB=BH...HF		HB=BH...HCl		HB=BH...HCN		HB=BH...H_2C_2		Assignment[c]
	ν	I	$\Delta\nu$	I	$\Delta\nu$	I	$\Delta\nu$	I	$\Delta\nu$	I	
ν_1			-404	1154(130)[b]	-328	1150(54)[b]	-114	379(79)[b]	-24	0(0)[b]	stret. of X–H
ν_2	1233	0	-3	0	-4	1	-2	0	-1	0	sym. stret. of B=B
ν_3	2838	20	10	9	7	10	7	3	2	15	anti-sym. stret. of B=B

[a] All frequencies (ν or $\Delta\nu$) are in cm^{-1} and IR intensities (I) are in km/mol
[b] The values in the parentheses are IR intensities of H–X stretching in isolated HX monomers and their frequencies are 4161, 3022, 3474 and 3538 cm^{-1}, respectively, and the values out of the parentheses are those of H–X stretching in the complexes
[c] Stret. stands for stretching

For comparison, we have also studied the T-shaped X–H...π hydrogen-bonded energies of the C_2H_4...HX complexes. The binding energy is evaluated to be 21.69, 16.40, 12.61 and 8.49 kJ/mol at MP2/aug-cc-PVTZ level for C_2H_4...HF, C_2H_4...HCl, C_2H_4...HCN and C_2H_4...H_2C_2, respectively. Comparing these results with the data listed in Table 3, it can be seen that the intermolecular T-shaped X–H...π hydrogen-bonded interaction in HB=BH...HX is stronger than that in $H_2C{=}CH_2$...HX, as is in accordance with the increment of the X–H bond distance.

As can be seen from Table 2, the binding energies obtained from MP2 and B3LYP methods at 6-311++G (2df,2p) and aug-cc-pVTZ levels are all in the same order of HB=BH...HF> HB=BH...HCl>HB=BH...HCN>HB=BH...H_2C_2, as is also in good agreement with the analyses of the H...π distance and the increment of the X–H bond.

The proportion of correlated interaction energies for the complexes to their total binding energies, defined as $[(-D_e)-(-D_{e(BSSE/ZPE)})]/(-D_e)$, are up to 16.93, 15.98, 8.68 and 4.36% at MP2/6-311++G(2df,2p), MP2/aug-cc-pVTZ, B3LYP/6-311++G(2df,2p) and B3LYP/aug-cc-pVTZ levels for BSSE corrections, respectively. This indicates the necessity of checking the BSSE corrections using MP2/6-311++G(2df,2p) and MP2/aug-cc-pVTZ methods for the interaction energies of the weak T-shaped X–H...π hydrogen bond. In particular, the ZPE corrections for the binding energies, which are up to 77.05, 74.40 and 85.27% at the MP2/6-311++G(2df,2p), B3LYP/6-311++G(2df,2p) and B3LYP/aug-cc-pVTZ levels, respectively, are larger than those of BSSE. Our previous investigations have shown that the ZPE corrections for the binding energies of the T-shaped X–H...π hydrogen-bonded interaction between $CH_3C{\equiv}N$ or $CH_3N{\equiv}C$ and H_2O, NH_3 or C_2H_2 are up to 54.32, 78.7 and 40.94% [17], and those between OCB≡BCO and HX are up to 40.28, 47.53, 56.83% [18], respectively. Furthermore, Ammal [14] has also claimed that the interaction energy was computed to be 3.1 kcal/mol at the MP2/6-311++G** level after correction of the BSSE while it was reduced to 1.4 kcal/mol after correction of the ZPEC and BSSE for C_2H_2...HF, suggesting that, for the weak T-shaped X–H...π hydrogen bond, the ZPE correction is very necessary for MP2 and B3LYP methods.

Vibration frequencies

The larger the frequency shifts, the more stable the complex is, so in this paper we showed some important frequency shifts in order to investigate the relative stabilities of the complexes. The most important vibrational frequency of proton donor, ν_1, can be approximately described as the stretching of X–H. From Table 3 it can be seen that the ν_1

Table 4 Calculated parameters of complexes at their equilibrium geometries: NBO occupation numbers for the B=B bands (Occ.(B=B)), the (X–H)* antibonds (Occ.(X–H)*), their respective orbital energies ε, the second-order perturbation energies $E^{(2)}$ and the sums of all atomic NBO charges of HX in their complexes (Q) at B3LYP/aug-cc-pVTZ level

	HB=BH...HF			HB=BH...HCl			HB=BH...HCN			HB=BH...H_2C_2		
Occ.(B=B)[a]	1.9258	$sp^{51.02}$	$sp^{51.02}$	1.9144	$sp^{66.45}$	$sp^{66.45}$	1.9765	$p^{1.00}$	$p^{1.00}$	1.9898	$p^{1.00}$	$p^{1.00}$
$\varepsilon\{(B=B)\}$[b]	-0.2394			-0.2301			-0.2320			-0.2174		
Occ.(X–H)*[a]	0.0700	$sp^{2.94}$		0.0821	$sp^{4.77}$		0.0313	$sp^{0.91}$		0.0134	$sp^{1.07}$	
$\varepsilon\{(X–H)^*\}$[b]	0.0700			0.0821			0.0313			0.0134		
$E^{(2)}_{(B=B)\rightarrow(X–H)^*}$[c]	20.84			17.14			4.69			2.04		
Q(H–X)	-0.0668			-0.0771			-0.0218			-0.0088		

[a] Occ.: occupation number
[b] In a.u
[c] In kcal/mol

decreased (red shifts) and the IR intensity increases greatly in complexes in comparison with those of the monomers, showing the formation of the X–H...π hydrogen-bonded interaction. The complex HB=BH...HF is the most stable one since there is the largest frequency shift in it (-404 cm^{-1}), while HB=BH...H_2C_2 is the most unstable one with the least frequency shift (only -24 cm^{-1}), as is consistent with the analyses of geometries and binding energies.

The ν_2 and ν_3 can be approximately described as the symmetrical stretching and anti-symmetrical stretching frequencies of the B=B bond, respectively. From Table 3, although the ν_2 decreased (red shifts) while the ν_3 increased (blue shifts), both of the frequencies changed more greatly in HB=BH...HF and HB=BH...HCl than those in HB=BH...HCN and HB=BH...H_2C_2, showing that the B=B...HF and B=B...HCl hydrogen bonds are strong while the B=B...H–C hydrogen bonds are weak, as is in accordance with the above analyses.

NBO analysis

To clarify the nature of the complexation, the NBO analysis was carried out. From Table 4 we can see that, for the boron atoms, the NBO approach mainly yields only one kind of hybridization which involves the formation of the T-shaped X–H...π hydrogen bond. It is almost of purely p (or mainly p) character and it is perpendicular to the molecular plane including the B–B bond to form the π-orbitals.

According to the NBO analysis, all the complexes have two units, as is in agreement with the character of most intermolecular interaction systems. In this study, delocalization effects between these two units can be identified from the presence of off-diagonal elements of the Fock matrix in the NBO basis, and the strengths of these delocalization interactions, $E^{(2)}$ [33], can be estimated by second-order perturbation theory. The results of $E^{(2)}$ indicate that in complex HB=BH...HF, the major interaction is that the B=B double bond offers the $sp^{51.02}$-hybridization π-electrons of the boron atoms to the contacting $\sigma_{(F–H)*}$ antibonding orbital of the HF and this T-shaped X–H...π hydrogen-bonded interaction has stabilized the system by 20.84 kcal/mol. Akin to HB=BH...HF, for complex HB=BH...HCl, the major interaction is $\pi_{B=B}\rightarrow\sigma_{(Cl–H)*}$, and it has stabilized the system by 17.14 kcal/mol. While in complexes HB=BH...HCN and HB=BH...H_2C_2, the B=B double bond offers the pure p electrons of π orbital to the $\sigma_{(C–H)*}$ antibonding orbital of the HCN or H_2C_2, and the T-shaped X–H...π hydrogen-bonded interaction is found where $E^{(2)}_{(B=B)\rightarrow(X–H)*}$ is 4.69 and 2.04 kcal/mol, respectively.

In the T-shaped OCB≡BCO…HX complexes, $E^{(2)}_{\pi(B\equiv B)\rightarrow\sigma(X–H)*}$ is 4.52, 3.56, 1.71 and 0.65 kJ/mol for OCB≡BCO...HF, OCB≡BCO...HCl, OCB≡BCO...HCN and OCB≡BCO...H_2C_2 at HF/aug-cc-PVTZ level, respectively [18]. Compared the result with the data listed in Table 4, it can be seen that the T-shaped X–H...π hydrogen-bonded interaction between the B=B double bond and HX is much higher than that between the B≡B triple bond and HX, as is agreement with the binding energies.

On the other hand, since the $E^{(2)}$ value from the $\pi_{(B=B)}\rightarrow\sigma_{(X–H)*}$ interaction is the order of HB=BH...HF>HB=BH...HCl>HB=BH...HCN>HB=BH...H_2C_2 and the net charge transfer is evaluated to be from HB=BH to proton donors by 66.8, 77.1, 21.8 and 8.3 me, respectively, the orders of the binding energy and stability are HB=BH...HF>HB=BH...HCl>HB=BH...HCN>HB=BH...H_2C_2, as is in accordance with the binding energies and geometries as well as frequencies analyses.

AIM analysis

It is well known that the electronic characteristics are very essential to reveal the nature of the hydrogen-bonded interactions. As an advanced method which can offer a simple, rigorous, and elegant way of partitioning any system into its atomic fragments, considering the gradient vector field of its electron density, the atoms in molecules theory (AIM) of Bader has been applied widely to study the hydrogen-bonded interactions for the complexes [35].

Our calculated AIM results show that, for each X–H...π contact, there is a bond path linking the hydrogen atom with the midpoint of the B=B bond accompanied by a bond critical point (see Fig. 1). Also, the values of the electron densities $\rho_{BCP(H...\pi)}$ obtained are within a range of 0.0075–0.0232 au (see Table 1), which fall into the common accepted values for H-bonds (0.002–0.04 au) [35], and the values of their Laplacians $\nabla^2\rho_{BCP}$ are all positive, indicating the typical closed-shell kind of interactions in the complexes. In other words, for all the X–H...π contacts, the small ρ_{BCP} and positive $\nabla^2\rho_{BCP}$ values are basically similar to the topological properties of normal weak X–H...π hydrogen bonds [35], thus suggesting the formation of T-shaped X–H...π hydrogen bond and confirming that the B=B double bond can be a potential proton acceptor. Additionally, the largest values of ρ_{BCP} and $\nabla^2\rho_{BCP}$ are predicted for the F–H...π interaction, reflecting the strongest F–H...π bond as noted above. On the other hand, the stronger X–H...π hydrogen bond in the complex HB=BH...HX than that in OCB≡BCO...HX is also observed from the larger electron densities $\rho_{BCP(H...\pi)}$ in the former than those in the latter, where the values of the electron densities $\rho_{BCP(H...\pi)}$ obtained are within a range of 0.0065–0.0149 au [18].

Bond intensity can be measured by ρ_{BCP}, where the fewer the ρ_{BCP} value, the less intensive the bond with the longer bond [35]. Here, to gain a deep insight into the origin of the B=B bond elongation, $\rho_{BCP(B=B)}$ calculations have also been

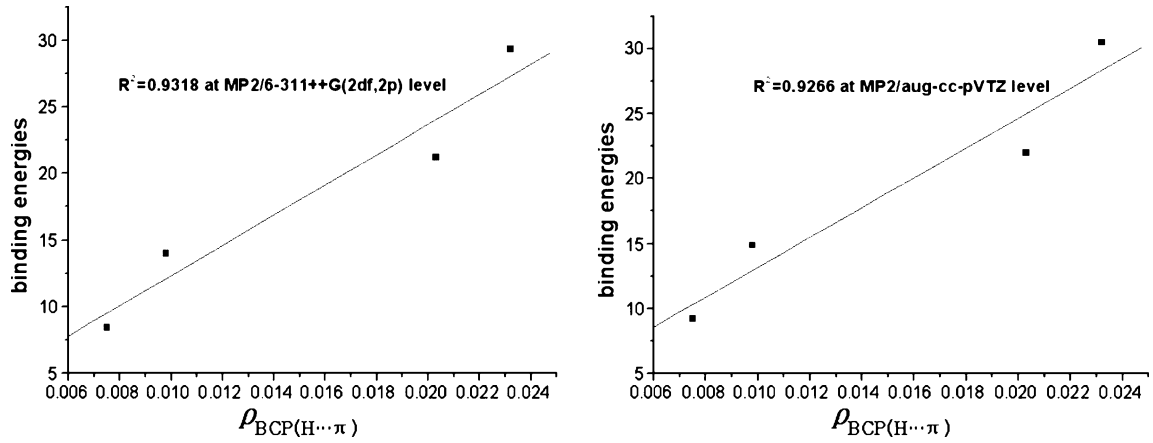

Fig. 2 The plot of binding energies versus $\rho_{BCP(H...\pi)}$

undertaken. Form Table 1, the $\rho_{BCP(B=B)}$ values in complexes, within a range of 0.1982–0.1992 au, are thinner than that in isolated HB=BH (0.1997 au), showing that the intensity of the B=B bond in complexes is weaker than that in monomer, i.e., B=B bond in complexes turn poorer, thus resulting in an elongation of the B=B bond. However, in the complexes OCB≡BCO...HX, the intensity of B≡B bond in complex is stronger than that in monomer, resulting in a contraction of the B≡B bond [18].

Interestingly, a good linear relationship is observed between the binding energies of the T-shaped hydrogen bond and the electron densities $\rho_{BCP(H...\pi)}$, and the correlation coefficient R^2 is up to 0.9318 and 0.9266 for the binding energies at MP2/6-311++G(2df,2p) and MP2/aug-cc-PVTZ levels, respectively (Fig. 2). As can be seen from Tables 1 and 2, HB=BH...HF has the least electron density $\rho_{BCP(B=B)}$ (0.1982) with the highest binding energies; in contrast, HB=BH...H_2C_2 has the most $\rho_{BCP(B=B)}$ (0.1992) with the poorest binding energy. It is known that changes in the electron density distribution in both the donor and acceptor molecules are the important consequence of hydrogen-bond formation [39]. So the change of electron density in both the donor and acceptor changes the strength of the T-shaped X–H...π hydrogen bond.

Analysis of the electron density shifts

Atomic charges are arbitrary by nature, and different schemes of partitioning electron density to one atom or another typically lead to discrepant charges [34]. Consideration of single molecular orbitals, whether delocalized or localized, can be misleading since they ignore all of the rest of the electrons. Maps of total electron density in space are not subject to such arbitrariness and therefore can be trusted to reveal density shifts with some fidelity [34].

To clarify the nature of the T-shaped X–H...π hydrogen-bonded interaction between HB=BH and HX in detail, the analysis of the electron density shifts that accompany formation of the X–H...π hydrogen-bonded interaction has been carried out. The shifts of electron densities are illustrated in Fig. 3. This map is generated by comparing the density in the complexes, point by point in space, to the same quantity in the isolated monomers. Purple regions of Fig. 3 hence represent the accumulation of additional electron density as a result of the mutual approach of the two molecules; yellow regions indicate loss of density.

The most obvious effects of the T-shaped H-bond formation are shown by the yellow region which is below the hydrogen atom of X–H bond, consistent with the accepted notion that the hydrogen loses density. The loss of

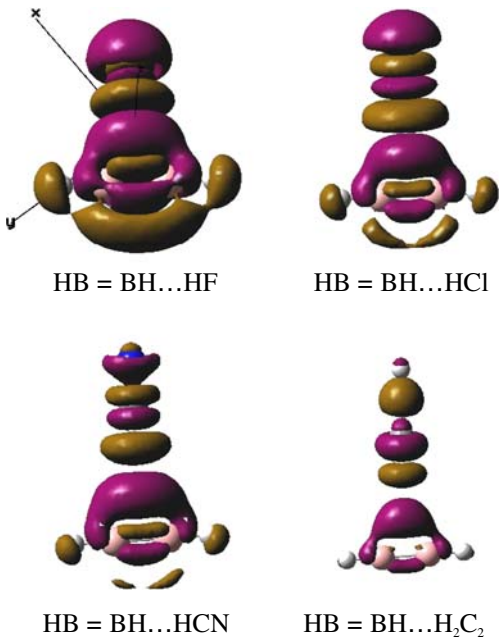

Fig. 3 Shifts of electron density as a result of formation of the complex between HX and HB=BH. Purple regions denote gain, and yellow regions represent loss

the hydrogen atom density weakens the X–H bond, leading to this bond elongation and the decrease of strength, as is in common with the feature of the conventional T-shaped H-bond.

Most important for our present consideration is the region along the B=B bond of the proton-accepting molecule. For each of the HB=B...HX complexes, it is apparent by the notable yellow region around the B=B bond axis that there is much charge loss of the B=B bond, accordance with the accepted notion that, due to the relative stronger fluidity of the π-electrons, the π-orbital of B=B bond tends to lose density. Much of this lost density is shifted toward the hydrogen atom of the proton donor, indicated by the large purple upbow-region above the yz-plane including the B=B bond, and little of density loss is shifted below the yz-plane (little purple area). Akin to the X–H bond, the loss of the density weakens B=B bond, leading to this bond elongation and the decrease of strength, as is in agreement with the analysis from the geometry.

Thus we can conclude that the nature of the T-shaped X–H...π hydrogen-bonded interaction is that much of the lost density from the π-orbital of B=B bond is shifted toward the hydrogen atom of the proton donor, leading to the electron density accumulation into the region above the yz-plane including the B=B bond and the formation of T-shaped X–H...π hydrogen-bond. Different from the B≡B bond contraction due to the increased density in B≡B bond tending to strengthen the bond [18], the B=B bond is elongated because of the electron density transferring from B=B bond to the hydrogen atom after complexation.

Conclusions

We performed calculations using MP2 and B3LYP methods at 6-311++G(2df,2p) and aug-cc-pVTZ levels for the singlet state HB=BH with HF, HCl, HCN and H_2C_2 systems. The unusual T-shaped X–H...π hydrogen bonds are found between the B=B double bond and the acid hydrogen. The binding energies follow the order of HB=BH...HF>HB=BH...HCl>HB=BH...HCN>HB=BH...H_2C_2. The hydrogen-bonded interactions in HB=BH...HX are found to be stronger than those in H_2C=CH_2...HX and OCB≡BCO...HX. The analyses of natural bond orbital (NBO) and the electron density shifts reveal that the nature of the T-shaped X–H...π hydrogen-bonded interaction is that much of the lost density from the π-orbital of B=B bond is shifted toward the hydrogen atom of the proton donor, leading to the electron density accumulation and the formation of the hydrogen bond. The atoms in molecules (AIM) theory have also been applied to characterize bond critical points and confirm that the B=B double bond can be a potential proton acceptor.

Acknowledgements The authors appreciate gratefully Professor Joel Liebman for the encouragement and the helpful advice and discussion.

References

1. Takahashi O, Kohno Y, Saito K (2003) Chem Phys Lett 378:509–515. doi:10.1016/S0009-2614(03)01173-4
2. Reynisson J, Steenken S (2003) J Mol Struct THEOCHEM 635:133–139. doi:10.1016/S0166-1280(03)00411-1
3. McDowell SAC (2001) Phys Chem Chem Phys 3:2754–2757. doi:10.1039/b102386c
4. Scheiner S, Grabowski SJ (2002) J Mol Struct 615:209–218. doi:10.1016/S0022-2860(02)00219-3
5. Tsuzuki S, Honda K, Uchimaru T, Mikami M, Tanabe K (2002) J Am Chem Soc 124:104–112. doi:10.1021/ja0105212
6. Sinnokrot MO, Valeev EF, Sherrill CD (2002) J Am Chem Soc 124:10887–10893. doi:10.1021/ja025896h
7. Sinnokrot MO, Sherrill CD (2004) J Phys Chem A 108:10200–10207. doi:10.1021/jp0469517
8. Park YC, Lee JS (2006) J Phys Chem A 110:5091–5095. doi:10.1021/jp0582888
9. DiStasio RA Jr, Steele RP, Rhee YM, Shao Y, Head-Gordon M (2007) J Comput Chem 28:839–856. doi:10.1002/jcc.20604
10. Rhee YM, DiStasio RA Jr, Lochan RC, Head-Gordon M (2006) Chem Phys Lett 426:197–203. doi:10.1016/j.cplett.2006.05.092
11. Podeszwa R, Bukowski R, Szalewicz K (2006) J Phys Chem A 110:10345–10354. doi:10.1021/jp064095o
12. DiStasio RA Jr, Helden GV, Steele RP, Head-Gordon M (2007) Chem Phys Lett 437:277–283. doi:10.1016/j.cplett.2007.02.034
13. Lopes KC, Araujo RCMU, Rusu VH, Ramos MN (2007) J Mol Struct 834-836:258–261. doi:10.1016/j.molstruc.2006.11.029
14. Ammal SSC, Venuvanalingam P (1998) J Chem Phys 109:9820–9830. doi:10.1063/1.477651
15. Tsuzuki S, Uchimaru T, Matsumura K, Mikami M, Tanabe K (2000) Chem Phys Lett 319:547–554. doi:10.1016/S0009-2614(00)00170-6
16. Ramos MN, Lopes KC, Silva WLV, Tavares AM, Castrini FA, Monte SAD et al. (2006) Spectrochim Acta Part A. Mol Biomol Spectrosc 63:383–390. doi:10.1016/j.saa.2005.05.024
17. Cao D, Ren F, Feng X, Wang J, Li Y, Hu Z et al (2008) J Mol Struct THEOCHEM 849:76–83. doi:10.1016/j.theochem.2007.10.018
18. Ren F, Cao D, Wang W, Wang J, Li Y, Hu Z et al (2008) Chem Phys Lett 455:32–37. doi:10.1016/j.cplett.2008.02.062
19. Knight LB Jr, Kerr K, Miller PK, Arrington CA (1995) J Phys Chem 99:16842–16848. doi:10.1021/j100046a009
20. Tague TJ, Andrews L (1994) J Am Chem Soc 116:4970–4976. doi:10.1021/ja00090a048
21. Ruščić B, Mayhew CA, Berkowitz J (1988) J Chem Phys 88:5580–5593. doi:10.1063/1.454569
22. Jouany C, Barthelat JC, Daudey JP (1987) Chem Phys Lett 136:52–56. doi:10.1016/0009-2614(87)87297-4
23. Sana M, Leroy G, Henriet C (1989) J Mol Struct THEOCHEM 187:233–250. doi:10.1016/0166-1280(89)85164-4
24. Curtiss LA, Pople JA (1989) J Chem Phys 91:4809–4812. doi:10.1063/1.456719
25. Treboux G, Barthelat JC (1993) J Am Chem Soc 115:4870–4878. doi:10.1021/ja00064a056
26. Perić M, Ostojić B, Engels B (1997) J Mol Spectrosc 182:280–294. doi:10.1006/jmsp.1996.7233
27. Perić M, Ostojić B, Engels B (1997) J Mol Spectrosc 182:295–308. doi:10.1006/jmsp.1996.7234
28. Xantheas SS, Dunning TH (1993) J Chem Phys 99:8774–8792. doi:10.1063/1.465599

29. Dunning TH Jr (2000) J Phys Chem A 104:9062–9080. doi:10.1021/jp001507z
30. Tanaka N, Tamezane T, Nishikiori H, Fujii T (2003) J Mol Struct THEOCHEM 631:21–28. doi:10.1016/S0166-1280(03)00129-5
31. Novoa JJ, Mota F (2000) Chem Phys Lett 318:345–354. doi:10.1016/S0009-2614(00)00016-6
32. Frisch MJ Trucks GA, Schlegel HB, Scuseria GE, Robb MA, Cheseman JR, Montgomery Jr JA, Vreeven T, Kudin KN, Burant JC, Millam JM, Iyengar SS, Tomasi J, Barone V, Mennuci B, Cossi M, Scalmani G, Rega N, Petersson GA, Nakatsuji H, Hada M, Ehara M, Toyota K, Fukuda R, Hasegawa J, Ishida M, Nakajima T, Honda Y, Kitao O, Nakai H, Klene M, Li X, Knox JE, Hratchian HP, Cross JB, Adamo C, Jaramillo J, Gomperts R, Stratmann RE, Yazyev O, Austin AJ, Cammi R, Pomelli C, Ochtersky JW, Ayala PY, Morokuma K, Voth GA, Salvador P, Dannenberg JJ, Zakrzewski VG, Dapprich S, Daniels AD, Strain MC, Farkas O, Malick DK, Rabuck AD, Raghavachari K, Foresman JB, Ortiz JV, Cui Q, Baboul AG, Clifford S, Cioslowski J, Stefanov BB, Liu G, Liashenko A, Piskorz P, Komaromi L, Martin RL, Fox DJ, Keith T, Al-Laham MA, Peng CY, Nanayakkara A, Challacombe M, Gill PMW, Johnson B, Chen W, Wong MW, Gonzalez C, Pople JA (2003) Gaussian 03, Revision B.03, Gaussian, Inc., Pittsburgh PA
33. Reed AE, Curtis LA, Weinhold FA (1988) Chem Rev 88:899–926. doi:10.1021/cr00088a005
34. Scheiner S, Kar T (2002) J Phys Chem A 106:1784–1789. doi:10.1021/jp013702z
35. Bader RFW (1990) Atoms in molecules, a quantum theory. Oxford University Press, New York
36. Biegler-König FW, Bader RFW, Tang TH (1982) J Comput Chem 3:317–328. doi:10.1002/jcc.540030306
37. Duijineveldt FB, van Duijineveldt-van de Rijdt JCM, Lenthe JHV (1994) Chem Rev 94:1873–1885. doi:10.1021/cr00031a007
38. Boys SF, Bernardi F (1970) Mol Phys 19:553–566. doi:10.1080/00268977000101561
39. Ebrahimi A, Roohi H, Habibi M, Hasannejad M (2006) Chem Phys 327:368–372. doi:10.1016/j.chemphys.2006.05.009